Title

Utrophin suppresses low frequency oscillations and coupled gating of mechanosensitive ion channels in dystrophic skeletal muscle

Journal

Channels, 9(3)

ISSN

1933-6950

Author

Lansman, Jeffry B

Publication Date

2015-05-04

DOI

10.1080/19336950.2015.1040211

Peer reviewed

Channels 9:3, 145–160; May/June 2015; © 2015 Taylor & Francis Group, LLC

Utrophin suppresses low frequency oscillations and coupled gating of mechanosensitive ion channels in dystrophic skeletal muscle

Jeffry B Lansman*

Department of Cellular and Molecular Pharmacology; School of Medicine; University of California San Francisco; San Francisco, CA USA

An absence of utrophin in muscle from *mdx* mice prolongs the open time of single mechanosensitive channels. On a time scale much longer than the duration of individual channel activations, genetic depletion of utrophin produces low frequency oscillations of channel open probability. Oscillatory channel opening occurred in the dystrophin/utrophin mutants, but was absent in wild-type and *mdx* fibers. By contrast, small conductance channels showed random gating behavior when present in the same patch. Applying a negative pressure to a patch on a DKO fiber produced a burst of mode II activity, but channels subsequently closed and remained silent for tens of seconds during the maintained pressure stimulus. In addition, simultaneous opening of multiple MS channels could be frequently observed in recordings from patches on DKO fibers, but only rarely in wild-type and *mdx* muscle. A model which accounts for the single-channel data is proposed in which utrophin acts as gating spring which maintains the mechanical stability a caveolar-like compartment. The state of this compartment is suggested to be dynamic; its continuity with the extracellular surface varying over seconds to minutes. Loss of the mechanical stability of this compartment contributes to pathogenic Ca^{2+} entry through MS channels in Duchenne dystrophy.

Keywords: calcium, calcium entry, Duchenne muscular dystrophy, dystrophin, mechanosensitive channel, muscular dystrophy, skeletal muscle, TRPV4, utrophin

*Correspondence to: Jeffry B Lansman; Email: jeff.lansman@ucsf.edu

Submitted: 03/23/2015

Revised: 04/02/2015

Accepted: 04/06/2015

http://dx.doi.org/10.1080/19336950.2015.1040211

Introduction

The dystrophin-associated glycoprotein complex in skeletal muscle links the extracellular matrix to the intracellular actin cytoskeletal network.[1-5] Contraction-induced stresses are generated both longitudinally as well as laterally. Lateral stresses disrupt alignment of sarcomeres and orientation of the t-tubular system, which reduce muscle force generation.[6-8] Evidence suggests the dystrophin-glycoprotein complex stabilizes lateral stresses by linking intracellular actin to laminin in the extracellular matrix at costameres, transverse circumferential structures overlying the Z bands.[8-10] In addition, skeletal muscle possesses excess membrane reserves such as caveolae, small dome-shaped indentations of the surface membrane, that prevent damage to the sarcolemma during muscle fiber elongation by providing a source of membrane when the fiber is stretched.[11]

Mutation in the dystrophin gene leads to the absence or reduced expression of dystrophin, which is the primary defect in Duchenne muscular dystrophy.[12-13] An early event in the pathogenesis of Duchenne dystrophy is an increase in intracellular Ca^{2+} levels as a result of increased Ca^{2+} influx across the cell membrane. There is now strong evidence showing mechanosensitive (MS) ion channels contribute to pathological Ca^{2+} entry in dystrophic skeletal muscle.[14-23] Recent work suggests MS channels in skeletal muscle are formed from TRPV4 proteins, although the precise subunit composition remains to be determined.[24]

The mechanisms by which MS channels transduce mechanical forces in skeletal muscle are only beginning to be understood. The simplest hypothesis is that dystrophin acts as a gating spring that controls membrane force transmission to MS channels. Alternatively, dystrophin may stabilize local membrane surface structure, composition, and/or geometry

through interactions with the sub-membrane actin cytoskeletal network. Other mechanisms are possible. It is clear, however, MS channels are part of a complex protein interactome, the muscle mechanosome, whose function depends on membrane lipid composition and bulk properties, as well as interactions between various cytoskeletal, scaffolding and signaling molecules. High time resolution recordings of single MS channels in muscle with genetic mutations in different components of the dystrophin-glycoprotein complex can provide insight into the mechanism of MS channel gating and the resulting changes in membrane Ca^{2+} fluxes which contribute to the pathogenesis of muscular dystrophy.

The *mdx* mouse lacks full-length dystrophin and has been used as a model for studying the pathogenesis of Duchenne dystrophy in humans.[25-27] The *mdx* mouse, however, has a rather mild disease compared with humans with Duchenne dystrophy. The reduced severity of disease in *mdx* mice is thought to be due to increased expression of utrophin, an autosomal gene product with significant homology to dystrophin.[28,29] In support of this idea, transgenic mice lacking both dystrophin and utrophin have severe muscle disease that more closely resembles Duchenne dystrophy[30,31] and increased transgenic expression of utrophin reduces the muscle pathology in the *mdx* mouse.[32,34]

In a preceding paper, we showed that genetic depletion of utrophin in muscle fibers from *mdx* mice produces a gene dose-dependent increase in the opening probability of single MS channels in recordings from membrane patches.[35] The increase in MS channel opening in the utrophin mutants lasted seconds rather than milliseconds. These openings, termed mode II activity, appeared as a sudden shift to high levels of channel activity followed by abrupt channel closure. Mode II activity was often followed by periods lasting tens of seconds to minutes in which channels remained silent. In addition, MS channels in utrophin mutants showed changes in single-channel conductance and subconductance state occupancy, suggesting dynamic coupling of individually gating channel subunits to form functional multimeric channels.[35]

In this paper, I describe MS channel gating in dystrophic muscle on a time scale that is much longer compared with the time course of individual MS channel activations. Time series analysis of MS channel activity reveals low frequency, periodic oscillations of MS channel open probability in *mdx* muscle lacking utrophin, but most prominently in muscle from double knockout (DKO) mice. The results also show cooperative or coupled gating of MS channels in which multiple channels open and close simultaneously. In some patches, exponential relaxation of the single-channel current preceded prolonged mode II activity. Relaxation of the single-channel current could be explained as dynamic changes in the access resistance to an MS channel-containing membrane domain. The data suggest a model in which dynamic changes in access to restricted membrane domains contribute to the changes in MS channel gating recorded from dystrophic muscle.

Results

Figure 1 shows a recording of single MS channel activity from a cell-attached patch on a wild type FDB fiber. **Figure 1a** shows single-channel currents representing ~16 s of continuous channel activity at a patch holding potential of –60 mV and the electrode pressure set to 0 mmHg. MS channel activity appears as short bursts of openings separated by longer closed periods.[15,23] The short horizontal bar at the top of the first record in **Figure 1a** indicates the burst of single-channel activity shown at the bottom on an expanded time scale. Single MS channel activity appears as rapid opening and closings with excursions to distinct subconductance levels.[23] **Figure 1b** shows the histogram of channel open times obtained by measuring channel open times using a threshold detection algorithm. The open time histogram was fitted as the sum of 2 exponential components using a maximum likelihood fitting routine. In this recording from a fiber from a wild-type mouse there was a major component with a time constant of 1.8 ms and a much smaller component with a time constant of 15 ms (see 35).

It is possible that the level of MS channel activity fluctuates over long time periods, either due to random variations in membrane mechanical properties or, perhaps, non-random forces generated by contractile elements or patch adhesion to the electrode.[36,37] Alternatively, MS channels may diffuse within the patch itself to the region where the cell membrane forms a seal with the electrode glass.[36] In the first set of experiments, I tested whether MS channel activity represents a simple stochastic process that is more or less constant over time using time series analysis of channel gating parameters. **Figure 1c** shows measurements of MS channel open probability as a function of time during the experiment. Each bar represents open probability measured during successive and equal intervals of time during ~5 minutes of a continuous recording. To analyze the correlation of channel open probability during successive time points, the autocorrelation function was calculated and plotted as a function of the lag *k*, the time interval between successive data points (details in Methods). **Figure 2d** shows the autocorrelation function had a simple form in which the autocorrelation is high for very short lags, but then drops to a low level and approaches zero as lag *k* increases. The form of the autocorrelation function indicates that there is little correlation between channel events with increasing separation in time and that gating of channel in wild-type muscle represents a stochastic process.

Figure 1e shows an experiment where I looked for correlation between channel open times measured in the same experiment. **Figure 1e** shows channel open times plotted sequentially as a function of time during the recording. There was no obvious grouping or abrupt changes in channel open times during the ~5 minute recording period. **Figure 1f** shows the autocorrelation function of channel open times as a function of the lag *k* between successive observations. The autocorrelation function of channel open times resembled that of open probability (**Fig. 1d**), except that open times showed somewhat more correlation at short lags. This likely reflects the fact that channels open as bursts in which each burst contains groups of individual openings.

Nonetheless, the autocorrelation function declined monotonically toward zero with increasing separation between observations as expected for a random gating process. In subsequent experiments, I restricted the analysis of autocorrelation to measurements of channel open probability to avoid experimental errors associated with incomplete openings and subconductance gating of MS channels.[23]

Figure 2 shows recordings of single MS channel activity that lasted several minutes on patches from an *mdx* and *mdx/utrn*$^{-/-}$ DKO muscle fiber. **Figure 2a** shows sequential 100 ms records of single-channel activity with the patch potential held at –60 mV and the electrode pressure set to 0 mmHg (*mdx* fiber, left records; DKO fiber, right records). The corresponding plots of channel open probability as a function of time during the recording are shown in **Figure 2b and c**. Note the prevalence of MS channel mode I activity in the *mdx* fiber. By contrast, MS channels in DKO muscle show both mode I and II activity. In **Figure 2c**, mode II activity in the DKO fiber begins during the fourth trace and continues during the fifth trace. The recording from the DKO fiber showed MS channels were open continuously for ~10 seconds and these periods of intense mode II activity were interspersed with low open probability mode I events. Subsequently, channels failed to open during the later half of the recording period. This could result from movement of the channel into an electrically isolated space such as a vesicle/membrane compartment or movement within the region where the cell membrane comes in contact with the recording electrode.[36] Alternatively, changes in membrane tension within the patch in the mutant may promote an inactivation or desensitization process, which occurs in the absence of an applied pressure stimulus.

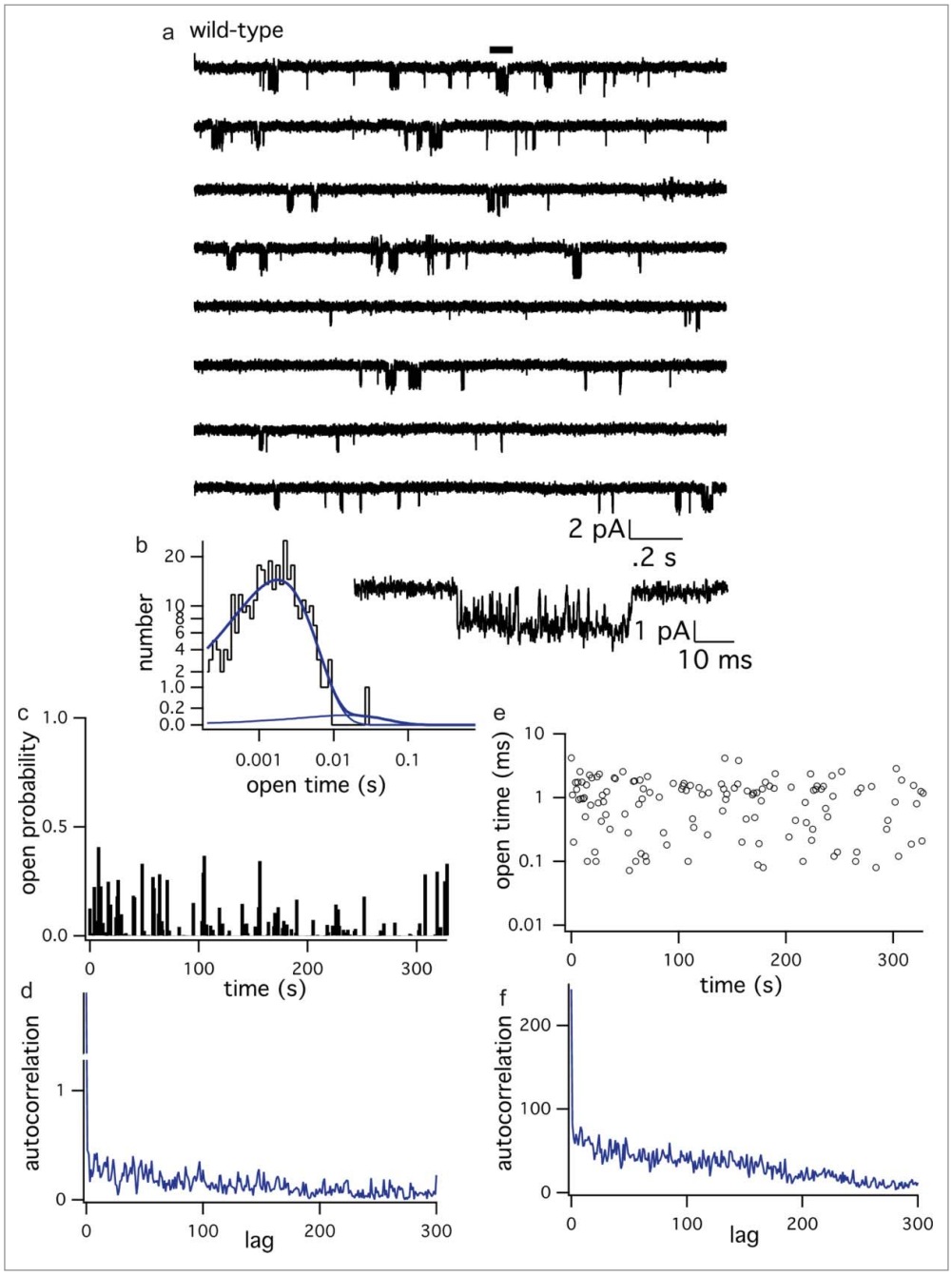

Figure 1. Time series analysis of MS channel activity recorded from a wild-type FDB fiber. (**a**) Single channel currents recorded from an FDB muscle fiber. The records represents ~20 seconds of continuous single-channel activity. The period of channel activity marked by horizontal bar is shown on an expanded time scale at the bottom of the records. Currents were sampled at 5 kHZ and filtered at 2 kHz. The single-channel conductance was 22 pS. The patch holding potential was –60 mV and the pressure in the electrode was set to 0 mmHg. (**b**) Histogram of MS channel open times. Data is from the same experiment as the records in (**a**). The open time distribution was fit as the sum of 2 exponential components with $\tau_o = 1.8$ and 15 ms, amplitudes 0.99 and 0.01. (**c**) Channel open probability plotted as a function of time during the recording. The data represents approximately 5 1/2 minutes of continuous channel activity at –60 mV. (**d**) Autocorrelation function of channel open probability (details in Methods). (**e**) MS channel open times plotted as a function of time during the recording. (**f**) Autocorrelation function of channel open times.

Figure 2d shows the autocorrelation function plotted as a function of lag *k* for channel open probability in the

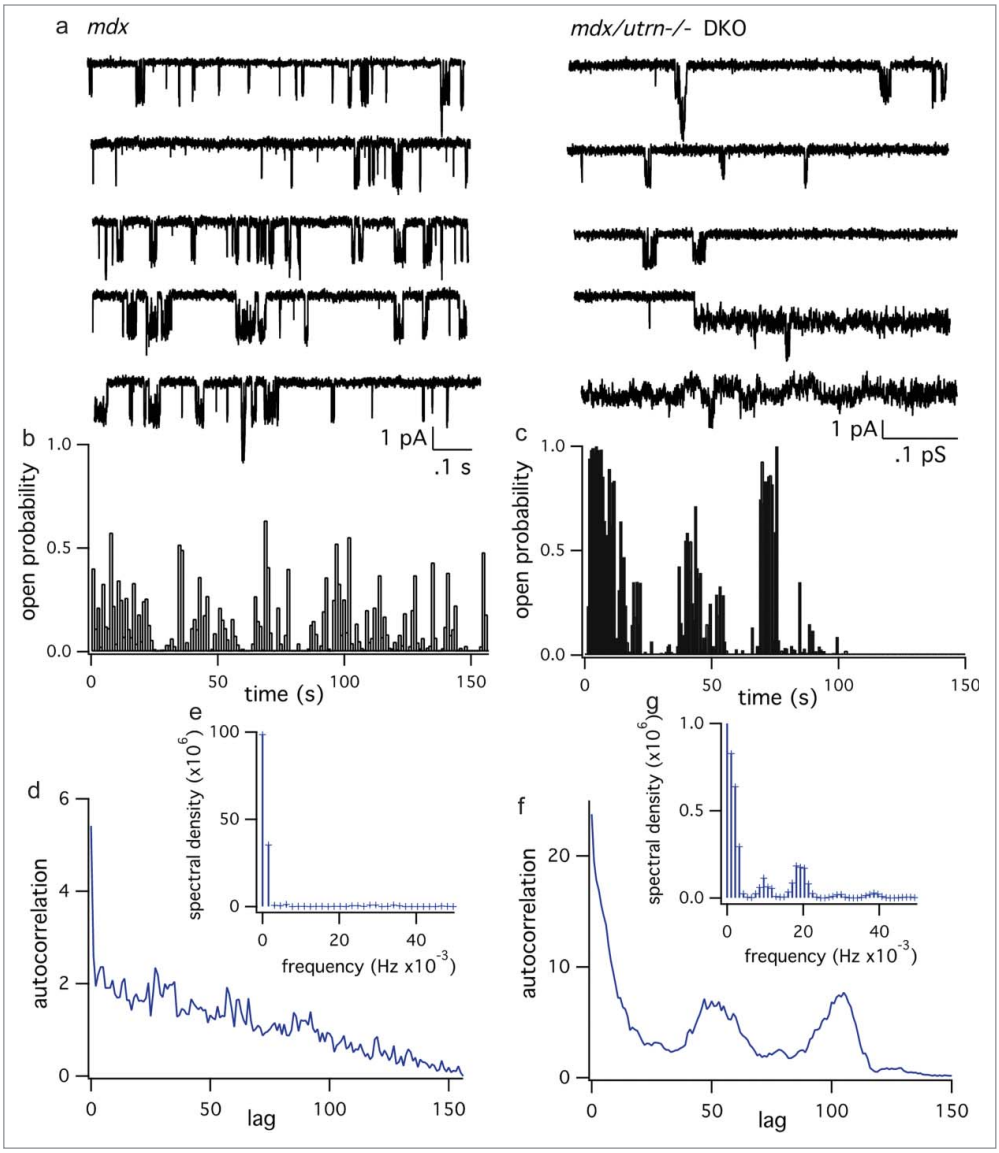

Figure 2. Time series analysis of MS channel open probability in *mdx* and *mdx/utrn*$^{-/-}$ DKO fibers. (**a**) Single-channel currents recorded from cell-attached patches from an *mdx* (left traces) and a DKO fiber (right traces. Note that MS channel currents showed only mode I gating in the *mdx* fiber, while in the DKO fiber there were both mode I and II openings. (**b**) MS channel open probability as a function of time during the recording from the *mdx* fiber. (**c**) MS channel open probability as a function of time during the recording from the DKO fibers. The figures represent ~2.5 minutes of continuous channel activity at a holding potential of –60 mV with the pipette pressure set to 0 mmHg. (**d**) Autocorrelation function of channel open probability as a function of time for channel activity in the *mdx* fiber plotted as a function of lag *k*. (**e**) Power spectra of the autocorrelation function of channel open probability vs time in the *mdx* fiber. (**f**) Autocorrelation function of channel open probability as a function of time in the DKO fiber plotted as a function of lag *k*. (**g**) Power spectra of the autocorrelation function in (**f**).

recording from the *mdx* fiber. The autocorrelation function decreased monotonically with increasing lag *k*, similar in form to that measured in recordings from wild-type fibers (**Fig. 1d**). However, the amplitude at every lag *k* was higher. The larger values of the autocorrelation function likely reflect the longer burst durations of MS channels in *mdx* compared with wild-type muscle.[23] **Figure 2f** shows the autocorrelation of MS channel open probability at increasing lag *k* in the DKO fiber. In this experiment, the autocorrelation function MS channel open probability is qualitatively different from that in wild-type or *mdx* fibers. The autocorrelation showed an initial maximum, but then declined; subsequently, it showed pronounced oscillations in amplitude with major peaks at lag $k = \sim 50$ and 100. **Figure 2g** shows the power spectrum of the autocorrelation function of MS channel open probability in the DKO fiber (**Fig. 2f**). There were 2 main peaks in the power spectrum at 0.01 and 0.02 Hz. There were also 2 minor peaks at somewhat higher frequencies. This differs from the power spectrum measured for channel activity in the *mdx* fiber, which was essentially flat (**Fig. 2e**). Evidently, gating of MS channels in DKO muscle over longer time periods shows periodic rather than a simple stochastic behavior.

Figure 3a compares MS channel activity recorded from 2 different patches on DKO fibers. The two patches differed in the pattern of MS channel activity. **Figure 3a** (left) shows a recording from a patch on a DKO fiber in which MS channels showed only mode I type activity. **Figure 3a** (right), by contrast, shows an example where MS channel activity consisted mostly of mode II events. These examples represent the variability in MS channel activity in different recordings of single-channel activity from membrane patches on DKO fibers.[35] Variability in MS channel gating in DKO muscle may reflect the spatial distribution of MS channels on the sarcolemma in relation to local membrane domains and/or proximity to cytoskeletal structures as well as variability in intrinsic patch tension and geometry. This issue is taken up in the Discussion.

Figure 3b and c shows MS channel open probability as a function of time during the recordings on the 2 DKO

fibers. **Figure 3b** shows that open probability in this experiment consisted entirely of low open probability mode I activity. **Figure 3c** shows a different pattern in which MS channel activity in the DKO appears almost exclusively as bursts of mode II activity separated by relatively long periods in there was no channel activity. **Figure 2d and c** show the autocorrelation function and power spectrum for the recording in which MS channel activity consisted primarily of mode I activity (**Fig. 1b**). Except for very short time intervals, there was little correlation of channel open probability as a function of lag *k*. This is reflected in the power spectrum (**Fig. 3e**), which was essentially flat. **Figure 3f** shows, by contrast, the autocorrelation function of channel open probability in the patch in which mode II activity dominated the single-channel activity. The autocorrelation function showed many large amplitude peaks. **Figure 3g** shows the power spectrum of the autocorrelation function. Over the frequency range shown there are at least 7 distinct peaks in the power spectra at frequencies between ~0.01–0.05 Hz. Evidently, mode II activity in DKO muscle is periodic. On the other hand, MS channel mode I activity in wild-type, *mdx*, or DKO muscle shows no evidence of periodicity and behaves more or less as a stochastic process. A tentative conclusion is that utrophin may act as a gating spring to dampen oscillations that arise from non-random changes in membrane tension and/or structure. However, the absence of utrophin is necessary but not sufficient to reveal periodic behavior. This suggests that utrophin may stabilize or interact with a tension-generating system such as the submembrane cytoskeleton.

We previously showed loss of a single utrophin allele in the *mdx/utrn*$^{-/-}$ heterozygotes produced an intermediate MS channel gating phenotype similar to that observed in DKO muscle, but with less frequent mode II activity.[35] Loss of a single utrophin allele also increased the probability of MS channel occupancy of small subconductance states in a manner similar to that seen in DKO muscle. These observations suggested that partial depletion of utrophin in heterozygotes would produce oscillatory mode II gating in some, but not all, patches. This was tested in the experiment shown in **Figure 4**.

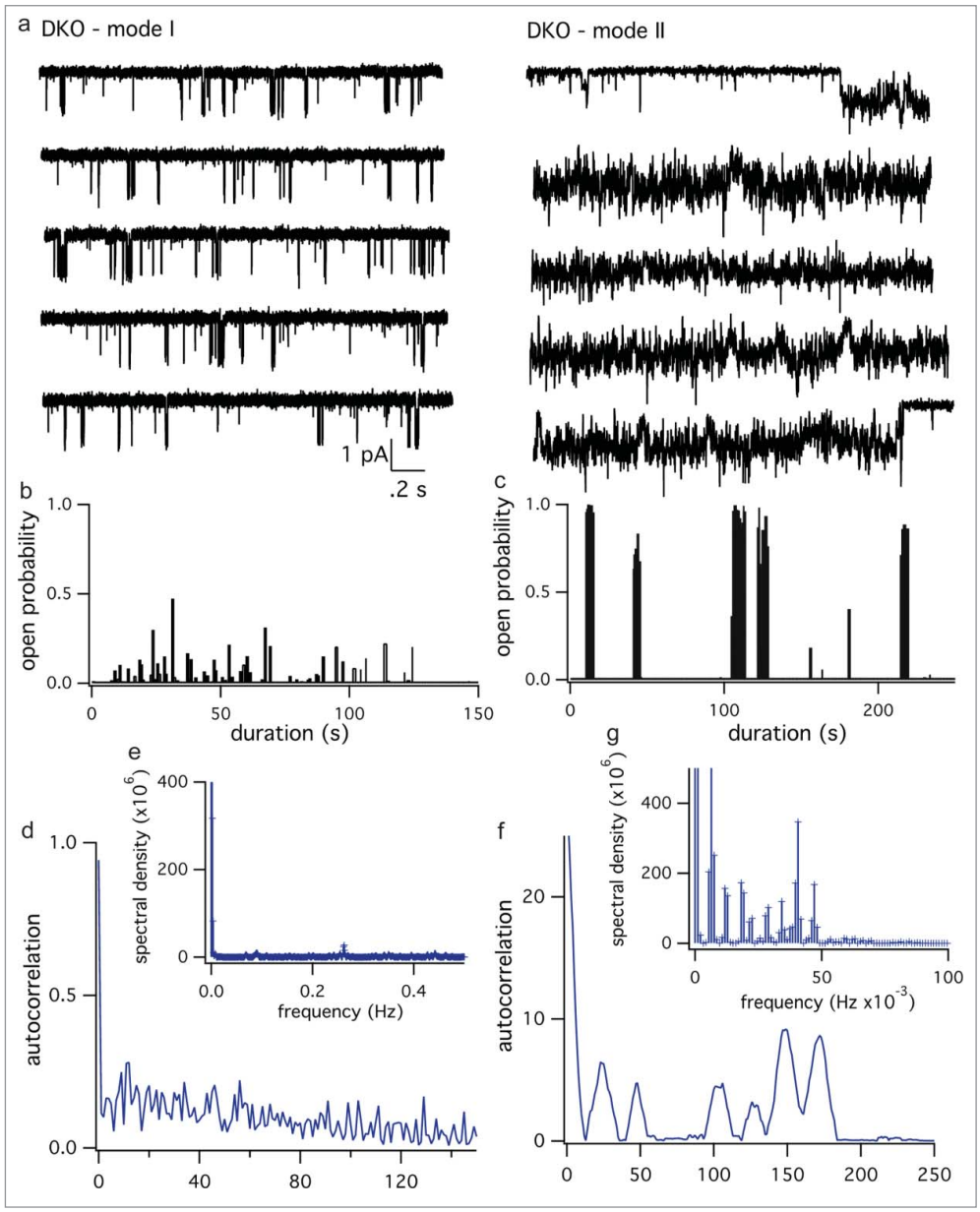

Figure 3. The autocorrelation function and power spectra for MS channel open probability in DKO fibers. (**a**) Single-channel currents recorded from a DKO fiber that exhibited primarily mode I gating (left records) or mode II gating (right records). (**b**) MS channel open probability plotted as a function of time during the recording for mode I gating in a DKO fiber. (**c**) MS channel open probability plotted as a function of time during the recording for mode II gating in a DKO fiber. (**d**) Autocorrelation function plotted as a function of lag *k* for the plot of DKO mode I open probability as a function of time during the recording. (**e**) Power spectra obtained from the autocorrelation function in (**d**). (**f**) Autocorrelation function plotted as a function of lag *k* for the plot of mode II gating of MS channels in a DKO fiber. (**g**) Power spectra of the autocorrelation function of mode II gating from (**e**). Note that mode II gating is associated with oscillations in the autocorrelation function and 6–7 discrete peaks in the power spectra.

Figure 4 shows the results obtained from 3 separate recordings on muscle fibers from *mdx*/utrophin heterozygotes. The top graphs (**Fig. 4a-c**) show MS channel open probability plotted as a function of time during each recording. **Figure 4d-f** show the corresponding autocorrelation functions and power spectra (insets) for the plots of open probability versus time. In 15 recordings from utrophin heterozygotes, only 3 patches showed oscillatory MS channel activity. **Figure 4f** is an example of a recording in which the autocorrelation function of channel open probability deviated from the simplest autoregressive model and exhibited periodicity. In this example, the oscillations appeared somewhat more compressed at lower frequencies and the peaks in the power spectra were sharper and had a smaller amplitude. On the other hand, the majority of patches on utrophin heterozygotes were similar to those shown in **Figure 4a and b**, in which the autocorrelation of open probability as a function of time showed little correlation between adjacent time points (**Figs. d,e**) and the power spectrum was flat (insets). Evidently, one utrophin allele is sufficient to suppress the highly periodic behavior of MS channels seen in DKO muscle.

Figure 5 summarizes the key findings of the time series analysis of MS channel gating in *mdx, mdx*/utrophin heterozygous, and DKO muscle. **Figure 5a** shows the fraction of patches in which MS channels showed periodic gating. Periodic activity was rare in recordings from *mdx* muscle (1/15). Periodic gating could be detected somewhat more frequently in utrophin heterozygotes (3/13), but was still relatively infrequent. The presence of mode II activity was, apparently, necessary but not sufficient to produce periodic gating in recordings from utrophin heterozygotes. On the other hand, ~70% of patches on DKO muscle with MS channel activity (8/12) showed periodicity that was highly correlated with the presence of mode II openings (data not shown). The results suggest the presence in muscle of a single utrophin allele is sufficient to suppress periodic mode II channel activity.

Figure 5b shows the combined results obtained from the spectral analysis of the autocorrelation function in all the recordings from utrophin heterozygotes and DKO fibers. The amplitude of each peak in the power spectrum for each experiment is plotted as a function of frequency. Open symbols represent experiments on utrophin heterozygotes; filled symbols represent experiments on DKO fibers. Different shaped symbols correspond to different experiments. The combined data show the spectral components of periodic gating were shifted toward lower frequencies in recordings from DKO muscle compared with utrophin heterozygotes. In addition, the amplitude of the spectral components tended to be greater in DKO muscle, although there was some variability, with one recording from a heterozygote showing relatively large amplitude spectral components. Taken together, however, the

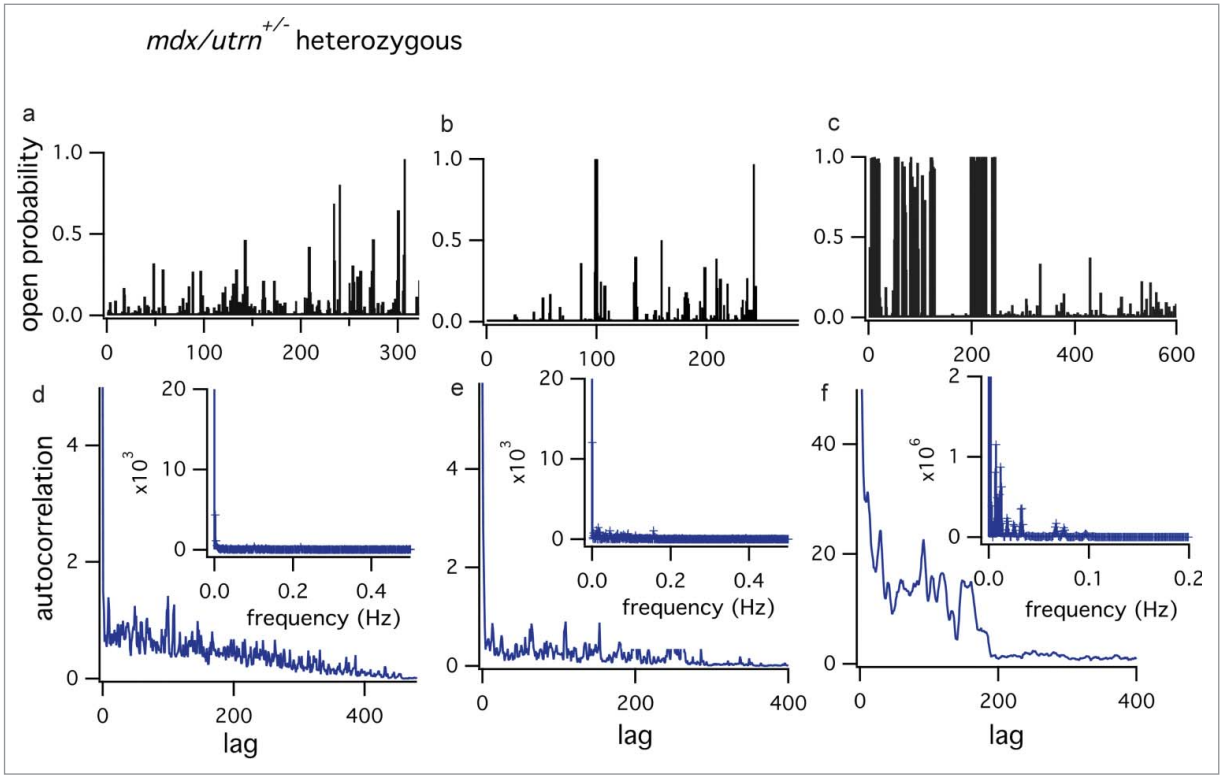

Figure 4. Time series analysis of MS channel open probability in *mdx/utrn*$^{+/-}$ heterozygous fibers. (**a–c**) Examples of MS channel open probability as a function of time during the recording for 3 different fibers from utrophin heterozygotes. (**d–f**) Autocorrelation function**s** and power spectra (insets) for the experiments shown in a-c. Note that peaks in the power spectra of MS channel gating in the utrophin heterozygotes are seen only when bursts of mode II gating are present as in (**c**).

results indicate complete loss of utrophin in DKO muscle unmasks low frequency oscillations of MS channel opening.

The effects of pressure on MS channel opening in utrophin mutants are complex. In some patches on DKO fibers, pressure activates MS channels, but the relationship between channel open probability and pressure is shifted to larger negative pressures compared with wild-type and *mdx* fibers (ref 35, **Fig. 6**). In other patches, however, pressure failed to increase channel open probability (not shown). One possibility is that the absence of both dystrophin and utrophin in DKO muscle renders MS channels more sensitive to an inactivation process. In this view, dystrophin/utrophin have a gating spring-like action which maintains membrane tension and prevents viscoelastic relaxations or other types of membrane changes that would alter mechanical force transduction through the membrane. Alternatively, the patch membrane on DKO fibers may be more compliant and/or have more labile infoldings of the surface membrane that absorb changes in patch tension.

In a number of patches on DKO muscle, MS channel activity was high at the beginning of the experiment, but then declined abruptly and the patch remained silent for the remainder of the recording period. This process was pronounced when the patch membrane was subjected to a constant pressure stimulus applied to the electrode. **Figure 6** shows an example of MS channel inactivation in response to the application of a constant pressure stimulus to the patch membrane. **Figure 6a** shows consecutive records of single MS channel activity. In this experiment, the patch electrode pressure was set to –20 mmHg shortly after seal formation and was held constant for ~2 minutes. The first 2 sweeps show characteristic mode I bursts of channel activity. Note that at the beginning of the third sweep (first asterisk) the inward single-channel current relaxes toward zero (second asterisk). The amplitude of the single-channel current subsequently increases again to the open state. The noise in the single-channel records likely reflects transitions between multiple subconductance states.[23,35]

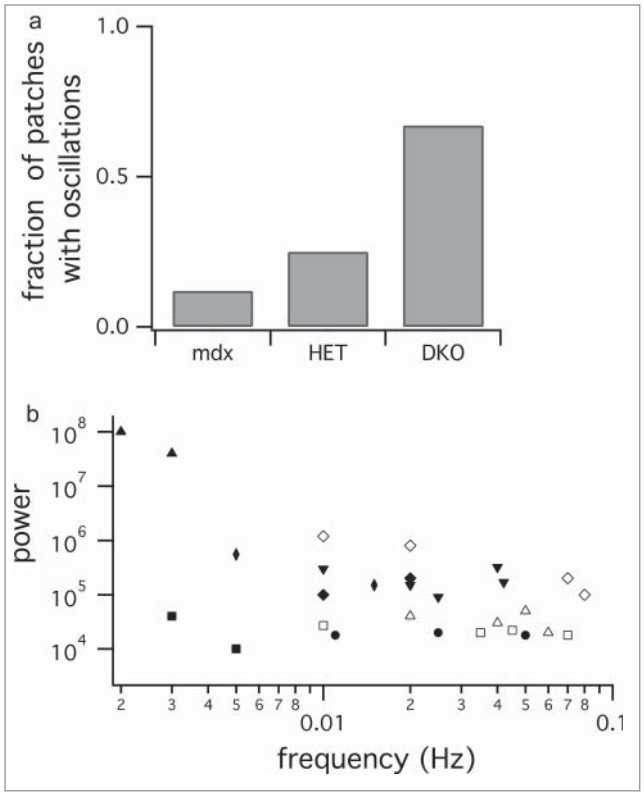

Figure 5. Spectral components of MS channel gating in *mdx, mdx/utrn*$^{+/-}$ heterozygotes, and DKO fibers. (**a**) Fraction of patches showing oscillations in the autocorrelation function of MS channel open probability. The values were 0.12, 0.25, and 0.67 for patches on *mdx, mdx/utrn*$^{+/-}$ heterozygotes, and DKO (n = 7, 12, and 13 patches, respectively). (**b**) Combined data from the analysis of the power spectra showing power as a function of frequency from analysis of open probability time series from heterozygous (open symbols) and DKO fibers (filled symbols). Each symbol is from a different patch. The recording from an *mdx* patch showing oscillatory behavior is off-scale, below the bottom of the y-axis and is not shown.

In this sweep and subsequent sweeps, the single-channel current decreased in amplitude, but recovered to the fully open state. In the last record, the channel returns abruptly to the closed state. **Figure 6b** shows channel open probability as a function of time during this recording, which lasted about a minute and a half. The bar at the top represents the period from which the records in **Figure 6a** were taken. Note that after the final closure, there is no MS channel activity for the remainder of the recording even though the pressure was held constant at –20 mmHg. Applying a larger pressure at later times also failed to elicit MS channel activity (data not shown). Artifacts such as irreversible formation of a membrane bleb in the electrode can be ruled out because it was possible to record voltage-activated Na^+ and K^+ currents in response to voltage steps (data not shown). Evidently, MS channel opening in response to pressure is transient and the channel does not reopen. The present experiments do not provide information on the precise mechanism for the loss of activity during maintained pressure. Additional experiments will be required to determine the relative role of channel properties and membrane mechanics in the observed inactivation process.

In a number of recordings from DKO muscle, the inward single-channel current showed a pronounced relaxation toward zero current. Often this relaxation preceded transition to mode II activity as shown in **Figure 6**a (asterisks). The time

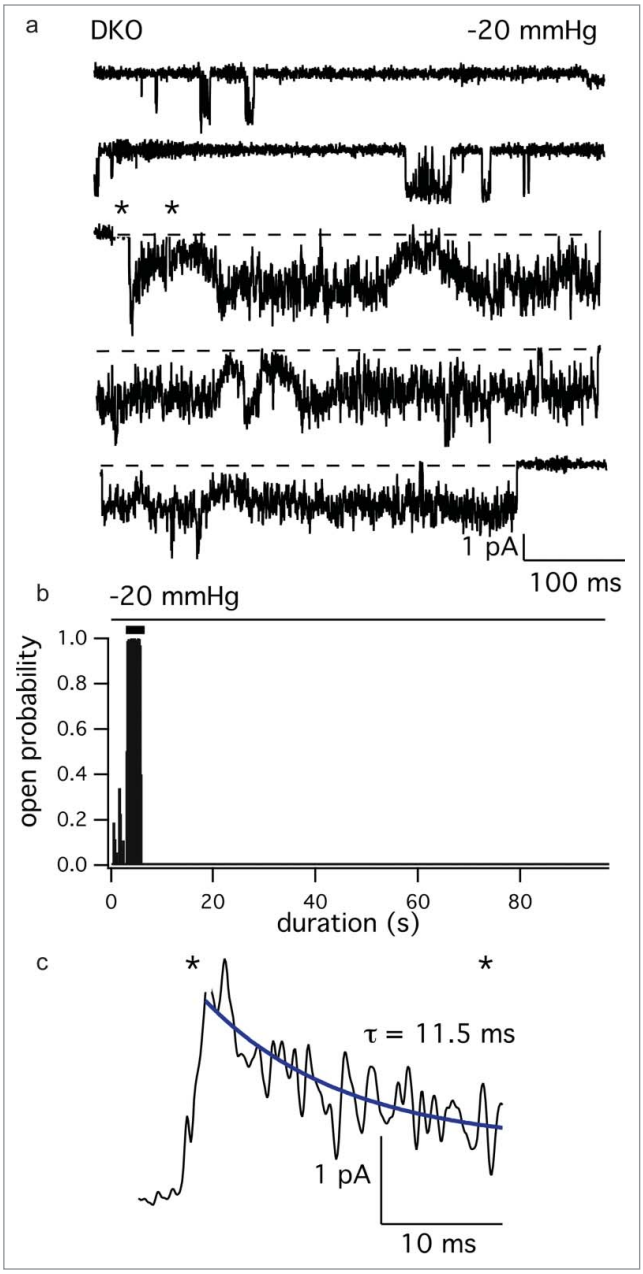

Figure 6. Inactivation of an MS channel showing mode II gating in a DKO fiber during maintained a pressure stimulus. (**a**) Records of single-channel activity recorded from a DKO fiber with the patch potential held at –60 mV and the pipette pressure set to –20 mmHg. The first 2 sweeps show channel opening occur initial as short mode I bursts followed by a period of mode II activity starting at the first asterisk in the third sweep. The channel returns to the closed state during the last sweep. Note the relaxation of the single-channel current from the open toward the closed state between the 2 asterisks at the beginning of sweep 3. (**b**) MS channel open probability plotted as a function of time with the pipette pressure set to –20 mmHg for the entire 100 seconds of this segment of channel activity. The bar above the period of high open probability represents the time period from which the sweeps in (a) were taken. Despite the maintained pressure stimulus, MS channel open probability was zero for the remaining time. (**c**) Analysis of the relaxation of the single channel current bewteen the 2 asterisks above sweep 3 in the records in (a). The current is shown inverted on a fast time scale and is fit with a single exponential with a time constant $\tau = 11.5$ seconds.

course of the inward current transient can not be explained by any obvious artifact, such as depolarization of the patch membrane potential, which would reduce the single-channel current by reducing the driving force for ion entry. In these experiments, the muscle fiber was bathed in an isotonic K^+ solution and so the muscle membrane potential is set to zero mV. On the other hand, a transient increase in a resistance that is in series with the patch membrane could give rise to an exponential current relaxation. In this case, a variable fraction of the applied voltage would fall across this series resistance. The source of such a series resistance is uncertain. The processes giving rise to the change in series resistance would have to be reversible because the single-channel current subsequently returns to the open level. A more trivial artifact involving irreversible formation of a membrane bleb within the patch electrode seems unlikely because single-channel activity persists for several seconds after the transient. In addition, single voltage-gated Na^+ and K^+ channels can be recorded al later times in the same patch when MS channels are silent (data not shown).

The inward current transient preceding mode II activity can be explained if it is assumed there is a membrane compartment that lies just beneath or is attached to the sarcolemma but remains electrically isolated from the extracellular surface. Such a compartment may correspond to a submembrane vesicle, such as those that insert glucose transporters into the sarcolemma or those involved in membrane repair mechanisms. Alternatively, the compartment may correspond to small caveolae in which the neck region that attaches the lumen to the sarcolemma is constricted or in a closed state.

Figure 6c shows the inward current transient inverted on an expanded time scale. The line through the current is the fit to a single exponential with a time constant $\tau = 11.5$ ms. The results in **Figure 6** suggest pressure may cause changes in the continuity of a submembrane compartment with the extracellular surface. Incorporation of such a compartment to the surface membrane would be expected to add additional surface area which could reduce tension in the membrane and lead to a reduction in MS channel activity. Although the present data is entirely consistent with such a hypothesis, additional experiments are clearly needed to establish a role of membrane trafficking events in MS channel gating.

Previous studies from this laboratory suggest that MS channels are multimeric proteins and individual subunits may be restricted in their spatial distribution to local membrane domains. Localization to membrane domains may account for both subconductance gating[23] as well as large conductance MS channels in utrophin mutants.[35] The next series of experiments investigated some possible consequences of the localization of MS channel subunits to restricted membrane domains in DKO muscle. **Figure** 7 shows that MS channels in DKO muscle undergo "coupled" gating in which the opening of more than one channel occurs simultaneously. **Figure** 7**a** shows records of MS channel activity recorded from a DKO fiber. Each record is ~1.8 seconds long. The patch potential was held at –60 mV and the electrode pressure was set to 0 mmHg. The first record shows characteristic mode I bursts in which the channel opens from the closed (c) to the fully open (o) state. At this compressed time scale, subconductance transitions are not resolved. The second record shows simultaneous opening and closing of 2 MS channels in the same recording. In this example, there is a single brief opening at the beginning of the record, followed by a transition from the closed state to an open level with an amplitude that is roughly twice the size of that in the first record. The two channels remain open and, subsequently, close simultaneously. Note, there are no closures from the doubly open state (o2) to the singly open level (o1). The graph below is an all points histogram of the amplitude of the single channel current for the entire recording, which included both the closed state and 2 open states (o1 and o2), each with an amplitude of ~ –1.4 pA. The "coupling ratio," which is a measure of the deviation from the binomial distribution, is 0.07 (See Methods for details). A coupling ratio << 1 indicates a high degree of coupling of the gating of individual MS channels in this patch.

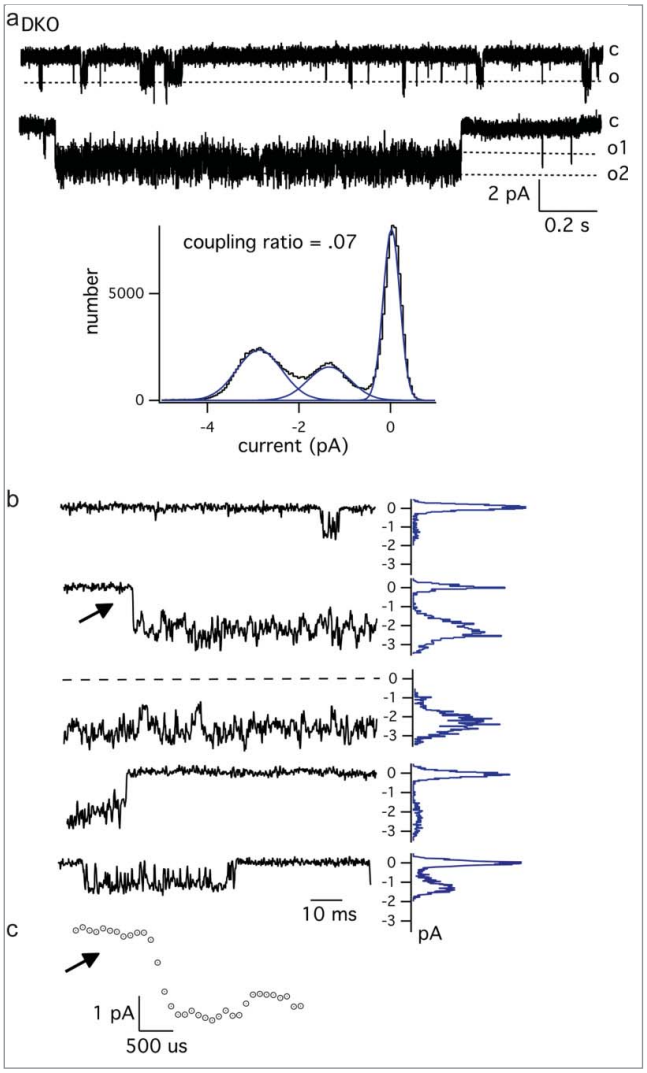

Figure 7. Coupled gating of MS channels in DKO muscle. (**a**) Single-channel currents recorded on a slow time scale from a DKO fiber. The patch potential was –60 mV and the pipette pressure was set to 0 mmHg. The top trace shows mode 1 bursts of single-channel openings. The bottom trace shows the simultaneous opening and closing of 2 channels each with a single-channel current i = ~1.4 pA. Below is the all point distribution of current amplitudes for the entire segment of channel activity which lasted ~2 minutes. The amplitude distribution was fit as the sum of 3 Gaussian components representing the closed state with a peak at 0 pA and either one or 2 channels fully open with amplitudes of –1.4 pA and –2.8 pA, respectively. (**b**) Records from the experiment in (a) shown on an expanded time scale. The graphs on the right show the all point distribution of current amplitudes for each trace of 100 ms. The arrow in trace 2 indicates the simultaneous opening of 2 channels and there is a corresponding shift in the open channel current to a value twice that of the first trace in which opening of only one channel is detected. The simultaneous opening of 2 channels persists until the fourth trace when both channels close. (**c**) The simultaneous open of 2 channels in trace 2 indicated with an arrow and shown at high time resolution. The two channels open simultaneously within ~500 μs.

Figure 7b shows records of MS channel activity from the same experiment, but on an expanded time scale. To the right of each record is the amplitude distribution of the single-channel current. The distribution is plotted with the axes switched so the *x*-axis is the number of points and the *y*-axis is the amplitude of the single-channel current (pA). The first record shows a brief mode 1 event. The amplitude distribution to the right shows a large peak at 0 pA corresponding to the closed channel current and a smaller peak at the fully open level of ~ –1.4 pA. The second sweep shows the simultaneous opening of 2 channels (arrow). The amplitude distribution to the right shows the open channel level is twice that of the first record

indicating simultaneous opening of 2 channels. The two channels remain open continuously and then close together following a somewhat slower time course than the opening transition in the fourth record. In the last record, only a single MS channel opens in a mode I burst. **Figure 7c** shows the simultaneous opening of 2 channels from **Figure 7b** at high time resolution. The arrow corresponds to the time of coupled opening in the record in **Figure 7b**. Note the 2 channels open within 500 μs, which is at the time resolution of the patch recording system. The single-channel current rises from the fully closed to the open level corresponding to 2 channels. At high resolution, it is not possible to discern opening of one channel prior to the other. Thus, coupled opening of MS channels in DKO muscle occurs within 500 μs. By contrast, MS channels in wild-type and *mdx* muscle often open by first passing through relatively long-lived subconductance states before reaching the fully open level.[23] In *mdx* muscle, in particular, the dwell time in a small subconductance state during opening can last 1–5 ms. Coupled opening of MS channels in **Figure 7** occurs almost 100 times faster than subconductance transitions between subunits.

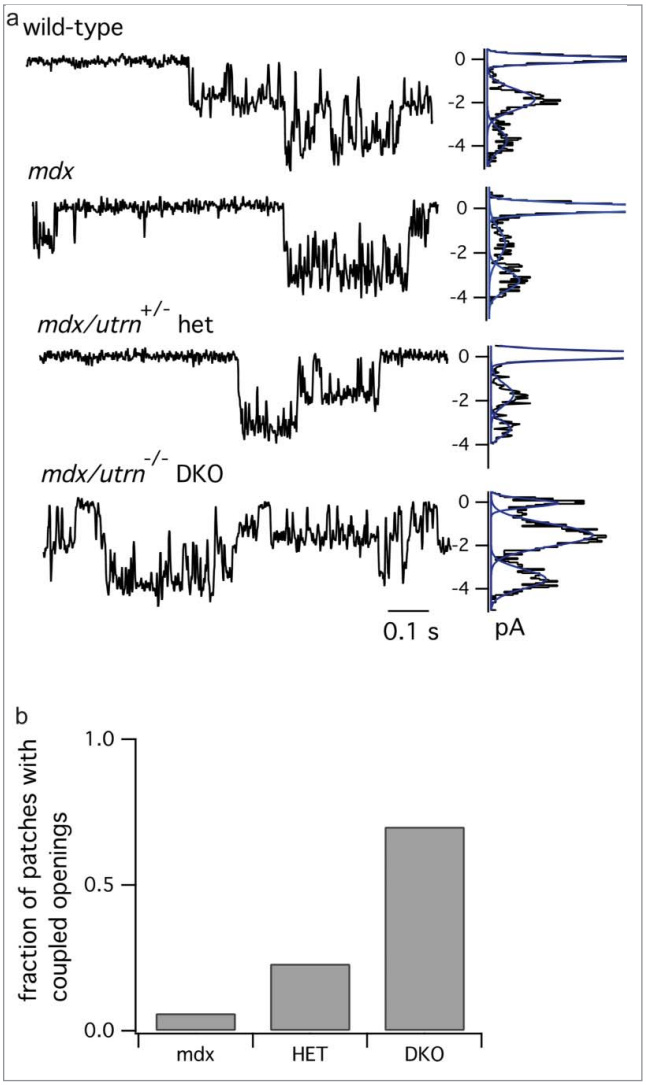

Figure 8. Coupled gating of MS channels in the different muscle genotypes. (**a**) Records of single-channel activity recorded from cell-attached patches on FDB fibers of the indicated genotypes. Each sweep is 100 ms. (**b**) Fraction of patches containing channels that gate in a cooperative manner. Wild-type fibers were not included because MS channel opening probability was low and there were insufficient points in the amplitude distribution corresponding to opening of 2 channels to calculate a coupling ratio.

Coupled gating was also detected in muscle isolated from mice of other genotypes. It occurred rarely in wild-type and *mdx* muscle and so there were insufficient numbers of coupled events during a recording to calculate a coupling ratio. In addition, global open probability was much lower in wild-type and *mdx* muscle than in the utrophin mutants so that most points in the amplitude histogram corresponded to the closed channel level. **Figure 8** shows examples of coupled gating of MS channels in wild-type, *mdx*, utrophin heterozygous and DKO muscle. In wild-type muscle, there was only weak coupling in that opening of the second channel did not occur simultaneously with the opening of the first channel. In the second record from an *mdx* fiber, channels open and closed simultaneously, although opening of the second channel occurred after a brief, but finite delay. In utrophin heterozygous (third record) and DKO muscle, openings and closings occurred more or less simultaneously, although during a portion of the record only one channel was open. **Figure 8b** shows the fraction of patches that showed coupled opening as determined by analysis of the all-points distribution of current amplitude. Wild-type recordings were not included because there were insufficient numbers of coupled events and long periods in which channels were closed. In *mdx* fibers, only 1/12 patches showed coupled gating; in heterozygotes, 2/14 showed coupled gating with coupling ratios of 0.03 and 0.2; in DKO muscle 6/12 patches showed coupled gating, with ratios 0.07, 0.14, 0.33, 0.4 (2 patches did not have sufficient points at the doubly open level to analyze the complete amplitude distribution. The conclusion that can be drawn is that a single utrophin allele is sufficient to suppress coupled gating in much the same manner as only a single utrophin allele is needed to suppress oscillatory gating.

In a previous paper,[35] we showed that a small conductance channel, which is likely TRPC1, shows greatly prolonged open times in utrophin mutants, but not wild-type or *mdx* muscle. Prolongation of the

open time depended on prior stimulation of the patch by applying a pressure stimulus. **Figure 9** shows an example of the induction of prolonged opening of the small conductance channel in response to a negative pressure applied to a patch on a DKO fiber that also contained an MS channel. **Fig. 9** (top) shows records of single-channel activity with –20, –30, –40, and –50 mmHg applied to the patch electrode. Note that applying pressure from –20 to –40 mmHg produced only a small change in MS channel opening consistent with a reduced sensitivity to pressure of MS channels in DKO muscle.[35] With a pressure stimulus of –50 mmHg opening of a smaller conductance channel can be seen. In this experiment the patch potential was –60 mV. **Figure 9b** shows the single-channel i-V relation for the small conductance channel and the slope gave a value of 7 pS.

After induction of the opening of the small conductance channel by the pressure stimulus, channels became highly active. **Figure 10** shows data from the same recording as **Figure 9**. **Figure 10a** shows sequential records of the opening and closing of 2 small conductance channels after the electrode pressure was returned to 0 mmHg. Note that channels open to either the o1 level or the o2 level where 2 channels were simultaneously open. **Figure 10b** shows the open probability of the small conductance channel plotted as a function of time during the recording, which lasted a little over 100 seconds. Since there are 2 channels present, the *y*-axis is the global open probability or Np_o. **Figure 10c and d** shows the autocorrelation function and power spectrum for the plot of channel open probability as a function of time in **Figure 10b**. The autocorrelation declines monotonically to zero with increasing lag *k* showing little periodicity. The larger values of the autocorrelation function at longer lags results from channel open times that are long compared to the duration of the time bin interval. This would produce a higher correlation between adjacent time points. The power spectrum is flat at all frequencies with no evidence of periodicity. The coupling ratio for the 2 channels in this experiment was calculated from the all points amplitude histogram (**Fig. 10e**).

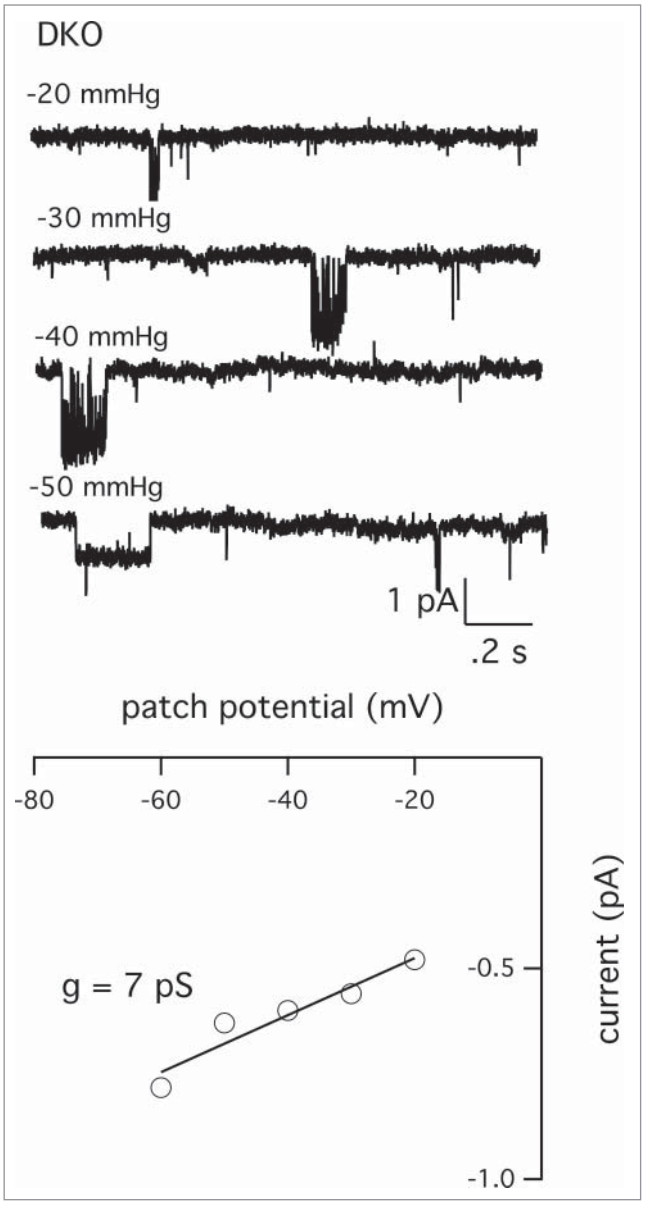

Figure 9. Effects of pressure on a patch containing both an MS channel and a small conductance channel. (Top) An example of a patch containing an MS channel (~22 pS) and a small conductance channel (7 pS). Note that increasing the pressure in the patch electrode produced only a small increase in MS channel opening in this patch. Applying pressures larger than ~30 mmHg was associated with appearance of the small conductance channel (bottom record at –40 mmHg). (Bottom) Single-channel current-voltage relation of the small conductance channel.

The amplitude histogram showed clear peaks corresponding to 0, 1 and 2 channels. The coupling ratio calculated from the areas under each peak of the amplitude histogram gave a value of 1.5. A coupling ratio greater than 1 indicates 2 independently gating channels with different open probabilities. The conclusion to be drawn is that small conductance channels show neither oscillatory nor coupled gating. This difference exists even when the 2 types of channels coexist in the same patch.

Discussion

This paper extends the analysis of MS channel gating behavior in DKO muscle to long time periods. The main findings

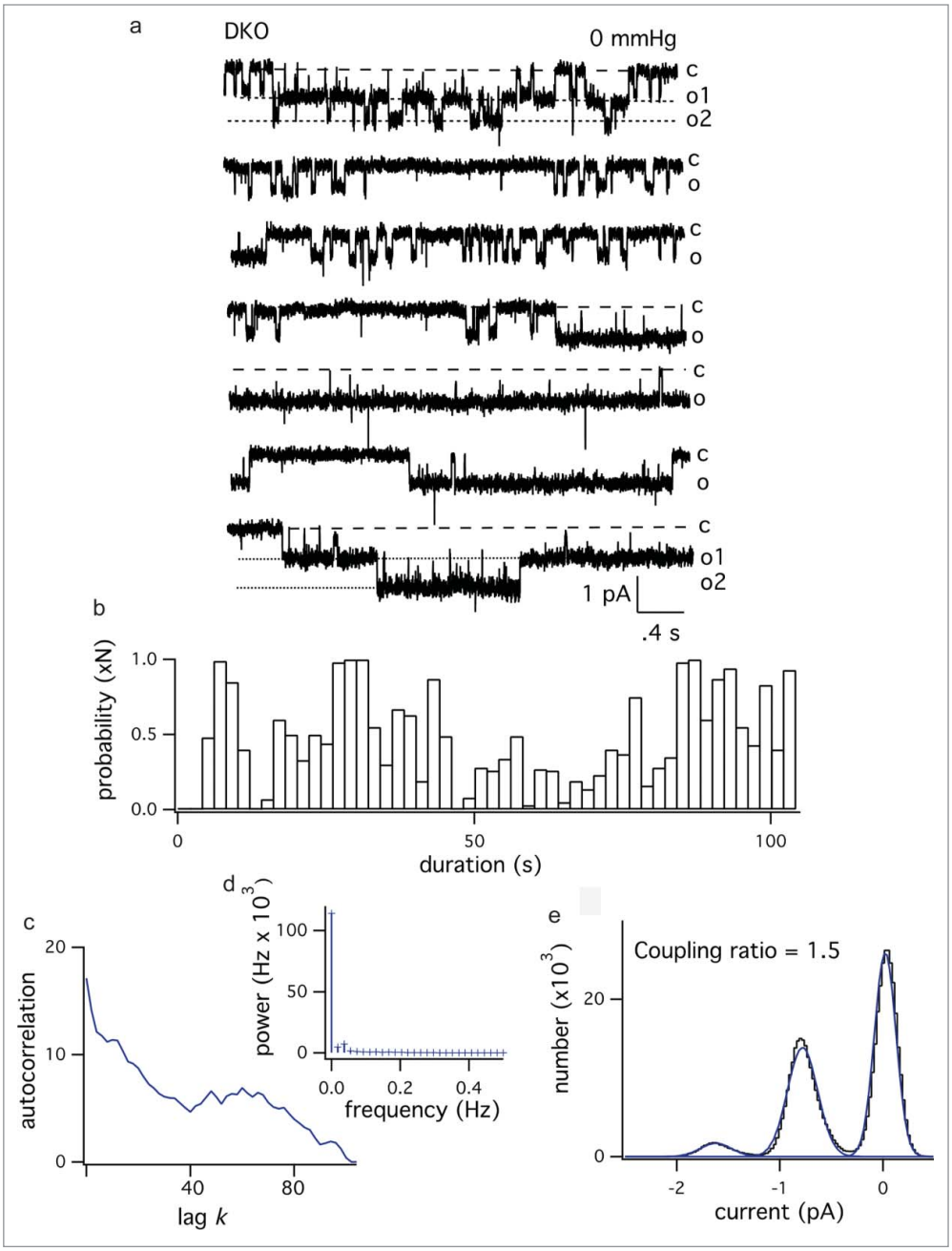

Figure 10. Time series analysis of small conductance channel gating in DKO muscle. The patch potential was –60 mV and the pressure was set to 0 mmHg. The data is from the same patch as **Figure 9**. (**a**) Records of single-channel activity of the small conductance channel showing multiple openings. Each sweep is ~4 seconds long. Note there appears to be one channel with a long open time and a second with a shorter open time. The sweeps are consecutive records. (**b**) Channel open probability plotted as a function of time for ~2 minutes of single-channel activity. Each bin corresponds to one sweep. (**c**) Autocorrelation function of channel open probability as a function of time plotted as a function of lag *k*. The autocorrelation function shows considerable persistence but drops monotonically to zero. The high degree of correlation at small lags represents the fact that channel open time is long compared to the bin width so that channel opening extends through several time bins. (**d**) Power spectra calculated from the autocorrelation function of channel open probability versus time. Note the power spectrum is flat showing no peaks in amplitude. (**e**) Distribution of the amplitude of the single-channel current in the entire recording which lasted ~2 minutes. The amplitude distribution was fit as the sum of 3 Gaussian components with peaks corresponding to 0, 1, or 2 channels open with peak amplitudes of –0.2, –0.8, and –1.6 pA and relative areas of 0.54, 0.41, and 0.05. The calculated coupling ratio was 1.5 indicating the presence of 2 independently gating channels having different open probabilities.

are as follows: (1) Genetic depletion of utrophin in muscle from dystrophin-deficient *mdx* mice produces periodic oscillations of MS channel open probability in ~70% of patches. (2) Applying a maintained pressure to the patch membrane on DKO fibers evokes a burst of MS channel opening lasting seconds. Bursts of mode II activity are often followed by a period of tens of seconds to minutes during which channels remain unavailable for opening. (3) Inward single-channel currents exhibit exponential relaxations toward zero current, suggesting dynamic changes in the access resistance of a membrane compartment. (4) MS channels in DKO muscle frequently exhibit coupled gating in which multiple channels open and close simultaneously. (5) Small conductance channels, which colocalize with MS channels in the same patch, fail to show either periodic oscillations in open probability or coupled gating. The discussion below considers the role of dystrophin/utrophin in the gating of MS channels and presents a simple mechanical model that reflects the known structural organization of the dystrophin-associated glycoprotein network and its interaction with the sarcolemma. Consideration will be given to the behavior of MS channels in wild-type, *mdx*, and DKO, since utrophin heterozygotes show an intermediate phenotype.[35] The intermediate phenotype of utrophin heterozygotes obscures salient features of mechanosome function revealed by complete depletion of utrophin in DKO muscle.

There is considerable variability in MS channel gating behavior in DKO muscle compared with wild-type and *mdx* muscle. MS channel activity may appear more or less exclusively as either mode

I or mode II activity (see **Fig. 3**, left and right records). Some patches, however, show both forms of channel activity. Mode II activity is generally periodic as shown by the autocorrelation function of channel open probability vs. time. In this paper, experiments were done with the patch pressure set to 0 mmHg. Under this condition, tension in the patch membrane depends primarily on adhesive forces between the membrane and glass electrode,[36,38] in addition to any membrane deformation forces produced by cytoskeletal elements.[20] The extent to which cytoskeletal forces contribute to membrane deformations in DKO muscle is unclear. It seems reasonable, however, to assume cytoskeletal elements exert mechanical forces on membrane patches, although the effects of these interactions are likely to vary in the different genotypes.

Variability in MS channel gating in DKO may reflect the fact that MS channels localize to spatially distinct regions of the sarcolemma. It seems unlikely oscillatory mode II activity reflects oscillatory changes in the concentration of a diffusible intracellular messenger, since the concentration of such a messenger would be expected to be more or less spatially uniform. Instead, it is assumed MS channels are more or less uniformly distributed, but that differences in channel behavior reflect the local membrane composition and surface morphology within the patch. For example, MS channels may be found both at costameric and extra-costameric locations. One possibility is that a population of MS channels is localized within costameric caveolae.[39] Because caveolae have a small radius of curvature, MS channels in caveolae will experience an intrinsically higher membrane tension than if they were embedded in flattened surface membrane and have a greater open probability. According to this view, variability in the extent of caveolar opening to the extracellular surface would produce variations in MS channel activity. Additionally, low activity MS channels may be localized to extra-caveolar sites.

The structural dynamics of the muscle membrane surface are poorly understood. Electron microscopic studies show caveolae as deep indentations of the plasma membrane or as more flattened structures.[11] Morphological studies have not been able to determine the extent to which caveolar continuity with the extracellular surface varies.[40] Moreover, there is little information on the extent to which the diameter of the caveolar neck region might vary over rapid time scales. **Figure 7** shows relaxation of the inward single-channel current that suggests formation of a compartment with high access resistance. The time constant of this relaxation would be determined by the constants of the series RC circuits that describe the membrane patch and compartment as wells as the series and seal resistances.[41]

A hypothetical model for modal gating of MS channels in DKO muscle is shown in **Figure 11**. Mode II activity occurs when the internal compartment becomes electrically continuous with the extracellular solution. In this case, mode II activity occurs via the increased membrane tension on the compartment because of its high radius of curvature. Alternatively, the lipid composition or presence of adaptor proteins may favor the open state. Upon flattening of the compartment so that it becomes continuous with patch membrane, changes in membrane tension favor mode I gating, which is largely determined by adhesive forces of the membrane patch. On the other hand, constriction of the neck connecting the membrane compartment to the surface would electrically isolate channels in the patch from the extracellular surface and lead to an absence of detectable single-channel activity (mode 0). It is also possible loss of channel activity represents diffusion of MS channels into the interface between the patch membrane and electrode.

The mechanism that gives rise to low frequency oscillations of MS channel open

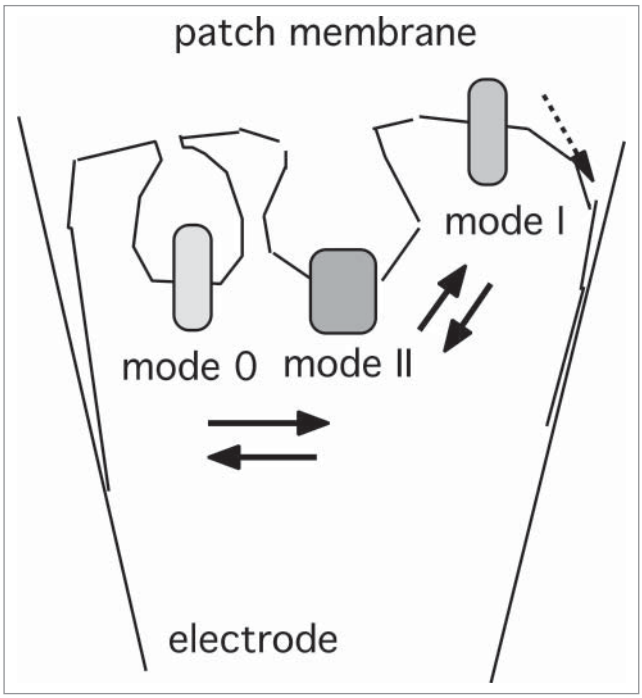

Figure 11. A simple compartment model for membrane dynamics associated with modal gating of MS channels in dystrophic muscle. In this diagram, MS channels are localized to either infolded membrane compartments with high (left) or low (right) access resistances or an expanded, flattened membrane. During silent periods (mode 0), MS channels are localized to a compartment that is electrically isolated from the cell surface. Upon expansion of the neck region of the compartment, continuity is established with the external surface and the composition and/or tension of the vesicular compartment favors prolonged opening (mode II). Flattening of the compartment and its incorporation into the patch membrane favors mode I gating. Alternatively, mode I gating occurs when the MS channels localize to the non-compartmentalized membrane. Loss of channel activity can also occur by diffusion of the channel into the interface between the membrane and glass electrode

probability is not known. Oscillations occur in the range of ~0.1 to ~.003 Hz (1 cycle every 10–200 seconds). These estimates were obtained during recordings lasting several minutes and so there could be even slower spectral components. It is unlikely low frequency oscillations represent the time course of the rise and fall of a chemical mediator, although the results cannot exclude such a process. Oscillations of MS channel activity may reflect dynamic mechanical processes within the patch membrane. This hypothesis is attractive because it suggests dystrophin/utrophin act as gating springs that dampen mechanical forces within the sarcolemma. Such forces may be produced by the actin/spectrin cytoskeletal network or by caveolin 3 and other structural/adaptor proteins. Association of dystrophin/utrophin with caveolae would suggest that loss of this interaction would render the membrane more susceptible to variations in tension associated that produce an instability of surface membrane invaginations in DKO muscle. Further studies are required to determine the role of utrophin on membrane domain structure and dynamics and its role in mechanotransduction.

Methods

Experimental animals

Experimental animals were identical to those described previously.[23,35] *Mdx* (C57BL/10Scn-*mdx*) mice were obtained from the Jackson Laboratory (Bar Harbour, ME, USA). Utrophin-deficient mice (strain B6.129-Utrntm1Jrs) were obtained from the Mutant Mouse Regional Resource Center (MMRRC) at the University of California, Davis. Double knockouts were obtained by breeding female *mdx* mice with male utrophin homozygotes. Male F1 offspring (X^{mdx} Y/$utrn^{+/-}$) were mated with *mdx* females (X^{mdx} X^{mdx}/$utrn^{+/+}$) giving an F2 generation of *mdx*/$utrn^{+/-}$ mice of both sexes. These mice were mated to produce *mdx*/$utrn^{-/-}$ DKOs; *mdx*/$utrn^{+/-}$ utrophin heterozygotes, *mdx*/$utrn^{+/+}$ utrophin wild-type. Genotyping was performed using PCR to identify the dystrophin mutation, the utrophin wild-type gene and the neomycin insert used to produce the utrophin transgenic knockout (Transnetyx Corp, Memphis, TN). Mice were sacrificed at 2–3 weeks of age. Methods for isolating single *flexor digitorum brevis* (FDB) muscle fibers were identical to those described in previous studies.[15,23,35] Dissociated fibers were incubated in oxygenated culture media at 34°C prior to use.

Electrophysiological methods

Single-channel currents were recorded with an EPC-9 patch clamp amplifier (HEKA Instruments, Southboro, MA) using Pulse® (HEKA) software for stimulus generation and data acquisition. Pressure was applied to the patch electrode using a pressure clamp device (HSPC-1, ALA Scientific). Patch electrodes were pulled from borosilicate capillaries and the tips heat polished to give a final resistance of ~1.5 – 1.7 MΩ with the electrode filled with normal saline and immersed in bathing solution containing isotonic K^+–aspartate.[15,16,23] The electrode solution contained (in millimolar): 150 NaCl, 5 KCl, 1 $MgCl_2$, 10 EGTA, 10 HEPES, and 17 glucose. The bathing solution contained (in millimolar): 150 potassium aspartate, 5 $MgCl_2$, 10 EGTA, 10 HEPES, and 10 glucose. The pH of both solutions was adjusted to 7.4 with TEA-OH. Single MS channel currents were recorded at a patch holding potential of –60 mV unless otherwise noted. At various times during a recording, voltage-activated Na^+ and K^+ currents were recorded in response to step changes in membrane potential from a holding potential of –90 mV. Macroscopic Na^+ and K^+ currents were obtained by averaging patch currents evoked by 10 identical voltage steps. Patch currents were digitized at either 2.5 or 50 kHz, filtered at 1 or 10 kHz, and stored directly on the hard disk of a Macintosh computer. Digitized currents were exported into IgorPro® (Wavemetrics, Portland, OR) or TAC® (Bruxton Corporation, Seattle, WA) for analysis.

Data analysis

MS channel open probability was measured in consecutive 100 ms segments as a function of time in recordings that lasted 1–5 minutes. Open probability was measured with TAC® event detection software using a half-threshold detection algorithm for event idealization. The autocorrelation function[42] was calculated to determine the extent of non-randomness of channel open probability during recordings that lasted minutes. Given sequential measurements of MS channel open probability, $Y_1, Y_2, \ldots, Y_N$ at times $X_1, X_2, \ldots, X_N$, the lag k autocorrelation function, r_k, is defined as

$$r_k = \frac{\sum_{i=1}^{N-k} \left(Y_i - \overline{Y}\right)\left(Y_{i+k} - \overline{Y}\right)}{\sum_{i=1}^{N} (Y_i - \overline{Y})^2}$$

where Y_i is the channel open probability at each time point and $\overline{Y}$ is the mean open probability over N observations. The autocorrelation function was plotted as a function of lag k. The autocorrelation was symmetrical for positive and negative values of k so only values for positive lag k are plotted. The 95% confidence limits of the autocorrelation function can be estimated as

$$2/\sqrt{N}$$

where N = the number of observations. The autocorrelation function at all values of lag k was well within this limit. A fast Fourier transform was performed on the autocorrelation function after correction for the number of time points to obtain the power spectra of the underlying time series. The amplitude and frequency of the major spectral components were obtained directly from the power spectra.

To examine the extent to which channels open cooperatively, I followed the procedure described by Porta et al to determine cooperative openings of ryanodine receptor channels in skeletal muscle.[43] As described in Porta et al, if there are N channels in a patch, each with an identical probability P_o of being in the open state, then the probability of finding n channels open at any given time (Φ_n) can be obtained from the binomial distribution

$$\Phi_n N!/n!(N-n)!P_o^n(-P_o)^{N-n}$$

where $\Sigma\ \Phi_n = 1$ and p_0 is the channel

open probability. To obtain Φ_n for each level of the single-channel current, the all-point distribution of current amplitudes is measured from a record of single-channel activity sufficiently long to have a sufficient number of points at each current level. It was generally not possible to obtain sufficient numbers of points in the amplitude histogram corresponding to multiple channel openings in wild-type and *mdx* muscle. This was because there were long periods in which channels were closed and openings were brief.

From the binomial distribution, it can be shown that

$$\Phi_n * \Phi_n / \Phi_{(n-1)} * \Phi_{(n+1)}$$

This term is independent of the open probability P_o of each individual channel. For an experiment in which there are 2 active channels in the patch (N = 0,1, and 2) the coupling ratio, CR, is defined as

$$CR = \Phi_1 * \Phi_1 * (k-1)/\Phi_0 * \Phi_{(2)} * 2k$$

When CR = 1, channels have identical open probabilities and open independently of one another; when CR >1, channels have different open probabilities and also gate independently; when CR < 1, channels open and close in a cooperative or coupled manner, with CR = 0 indicating all channels open and close simultaneously and indistinguishable from the gating of a single channel protein with twice the unitary conductance.

Disclosure of Potential Conflicts of Interest

No potential conflicts of interest were disclosed.

Acknowledgments

The author thanks Dr Nhi Tan for expert technical assistance during the early experiments.

Funding

Supported by a grant from the Krasnow Foundation.

References

1. Porter GA, Dmytrenko GM, Winkelmann JC, Bloch RJ. Dystrophin colocalizes with beta-spectrin in distinct subsarcolemmal domains in mammalian skeletal muscle. J Cell Biol 1992; 117(5):997-05; PMID:1577872; http://dx.doi.org/10.1083/jcb.117.5.997
2. Ervasti JM, Campbell KP. Membrane organization of the dystrophin-glycoprotein complex. Cell 1991; 66 (6):1121-31; PMID:1913804; http://dx.doi.org/10.1016/0092-8674(91)90035-W
3. Ervasti JM, Campbell KP. A role for the dystrophin-glycoprotein complex as a transmembrane linker between laminin and actin. J Cell Biol 1993; 122 (4):809-23; PMID:8349731; http://dx.doi.org/10.1083/jcb.122.4.809
4. Williams MW, Bloch RJ. Extensive but coordinated reorganization of the membrane skeleton in myofibers of dystrophic (mdx) mice. J Cell Biol 1999; 144 (6):1259-70; PMID:10087268; http://dx.doi.org/10.1083/jcb.144.6.1259
5. Rybakova IN, Patel JR, Ervasti JM. The dystrophin complex forms a mechanically strong link between the sarcolemma and costameric actin. J Cell Biol 2000; 150 (5):1209-14; PMID:10974007; http://dx.doi.org/10.1083/jcb.150.5.1209
6. Street SF. Lateral transmission of tension in frog myofibers: a myofibrillar network and transverse cytoskeletal connections are possible transmitters. J Cell Physiol 1983; 114:346-64; PMID:6601109; http://dx.doi.org/10.1002/jcp.1041140314
7. Brown LM, Hill L. Some observations on variations on filament overlap in tetanized muscle fibres and fibres stretched during a tetanus, detected in the electron microscope after rapid fixation. J Musc Res Cell Mot 1991; 12:171-82; http://dx.doi.org/10.1007/BF01774036
8. Bloch R, Gonzalez-Serratos H. Lateral force transmission across costameres in skeletal muscle. Exerc Sport Sci Rev 2003; 31(2):73-8; PMID:12715970; http://dx.doi.org/10.1097/00003677-200304000-00004
9. Pardo JV, Siliciano JD, Craig SW. A vinculin-containing cortical lattice in skeletal muscle: transverse lattice elements ("costameres") mark sites of attachment between myofibrils and sarcolemma. Proc Natl Acad Sci U S A 1983; 80(4):1008-12; PMID:6405378; http://dx.doi.org/10.1073/pnas.80.4.1008
10. Craig SW, Pardo JV. Gamma actin, spectrin, and intermediate filament proteins colocalize with vinculin at costameres, myofibril-to-sarcolemma attachment sites. Cell Motil 1983; 3(5-6):449-62; PMID:6420066; http://dx.doi.org/10.1002/cm.970030513
11. Dulhunty AF, Franzini-Armstrong C. The relative contributions of the folds and caveolae to the surface membrane of frog skeletal muscle fibres at different sarcomere lengths. J Physiol 1973; 250(3):513-39; http://dx.doi.org/10.1113/jphysiol.1975.sp011068
12. Hoffman EP, Brown RH Jr, Kunkel LM. Dystrophin: the protein product of the Duchenne muscular dystrophy locus. Cell 1987; 51(6):919-28; PMID:3319190; http://dx.doi.org/10.1016/0092-8674(87)90579-4
13. Bonilla E, Samitt CE, Miranda AF, Hays AP, Salviati G, DiMauro S, Kunkel LM, Hoffman EP, Rowland LP. Duchenne muscular dystrophy: deficiency of dystrophin at the muscle cell surface. Cell 1988; 54 (4):447-52. PMID:3042151; http://dx.doi.org/10.1016/0092-8674(88)90065-7
14. Franco A Jr, Lansman JB. Calcium entry through stretch-inactivated ion channels in mdx myotubes. Nature 1990; 344: 670-73; PMID:1691450; http://dx.doi.org/10.1038/344670a0
15. Franco-Obregón A, Lansman JB. Mechanosensitive ion channels in skeletal muscle from normal and dystrophic mice. J Physiol 1994; 481(Pt 2):299-09; http://dx.doi.org/10.1113/jphysiol.1994.sp020440
16. Franco-Obregón A, Lansman JB. Changes in mechanosensitive channel gating following mechanical stimulation in skeletal muscle myotubes from the mdx mouse. J Physiol 2002; 539(Pt 2):391-47; http://dx.doi.org/10.1113/jphysiol.2001.013043
17. De Backer F, DeBacker C, Gailly P, Gillis JM. Long-term study of Ca^{2+} homeostasis and of survival in collagenase-isolated muscle fibres from normal and *mdx* mice. J Physiol 2002; 542(Pt 3):855-65; PMID:12154184; http://dx.doi.org/10.1113/jphysiol.2002.020487
18. Allen DG, Whitehead NP, Yeung EW. Mechanisms of stretch-induced muscle damage in normal and dystrophic muscle: role of ionic changes. J Physiol 2005; 567.3:723-35; http://dx.doi.org/10.1113/jphysiol.2005.091694
19. Yeung EW, Whitehead NP, Suchyna TM, Gottlieb PA, Sachs F, Allen DG. Effects of stretch-activated channel blockers on $[Ca^{2+}]_i$ and muscle damage in the *mdx* mouse. J Physiol 2005; 562(Pt 2):367-80; PMID:15528244; http://dx.doi.org/10.1113/jphysiol.2004.075275
20. Suchyna TM, Sachs F. Mechanosensitive channel properties and membrane mechanics in mouse dystrophic myotubes. J Physiol 2007; 15; 581(Pt 1):369-87
21. Teichmann MD, Wegner FV, Fink RH, Chamberlain JS, Launikonis BS, Martinac B, Friedrich O. Inhibitory control over Ca(2+) sparks via mechanosensitive channels is disrupted in dystrophin deficient muscle but restored by mini-dystrophin expression. PLoS One 2008; 3(11):e3644; PMID:18982068; http://dx.doi.org/10.1371/journal.pone.0003644
22. Khairallah RJ, Shi G, Sbrana F, Prosser BL, Borroto C, Mazaitis MJ, Hoffman EP, Mahurkar A, Sachs F, Sun Y, et al. Microtubules underlie dysfunction in duchenne muscular dystrophy. Sci Signal 2012; 5(236): ra56; PMID:22871609; http://dx.doi.org/10.1126/scisignal.2002829
23. Vasquez I, Tan N, Boonyasampant M, Koppitch KA, Lansman JB. Partial opening and subconductance gating of mechanosensitive ion channels in dystrophic skeletal muscle. J Physiol 2012; 590(Pt 23):6167-85; PMID:22966155; http://dx.doi.org/10.1113/jphysiol.2012.240044. Epub 2012 Sep 10
24. Ho TC, Horn NA, Huynh T, Kelava L, Lansman JB. Evidence TRPV4 contributes to mechanosensitive ion channels in mouse skeletal muscle fibers. Channels (Austin) 2012; 6(4):246-54; PMID:22785252; http://dx.doi.org/10.4161/chan.20719
25. Dangain J, Vrbova G. Muscle development in mdx mutant mice. Muscle Nerve 1984; 7(9):700-4. PMID:6543918; http://dx.doi.org/10.1002/mus.880070903
26. Tanabe Y, Esaki K, Nomura T. Skeletal muscle pathology in X chromosome-linked muscular dystrophy (mdx) mouse. Acta Neuropathol 1986; 69(1-2):91-5. PMID:3962599; http://dx.doi.org/10.1007/BF00687043
27. Carnwath JW, Shotton DM. Muscular dystrophy in the mdx mouse: histopathology of the soleus and extensor digitorum longus muscles. J Neurol Sci 1987; 80 (1):39-54. PMID:3612180; http://dx.doi.org/10.1016/0022-510X(87)90219-X
28. Love DR, Hill DF, Dickson G, Spurr NK, Byth BC, Marsden RF, Walsh FS, Edwards YH, Davies KE. An autosomal transcript in skeletal muscle with homology to dystrophin. Nature 1989; 339(6219):55-8. PMID:2541343; http://dx.doi.org/10.1038/339055a0
29. Tinsley JM, Blake DJ, Roche A, Fairbrother U, Riss J, Byth BC, Knight AE, Kendrick-Jones J, Suthers GK, Love DR, et al. Primary structure of dystrophin-related protein. Nature 1992; 360(6404):591-3. PMID:1461283; http://dx.doi.org/10.1038/360591a0
30. Deconinck AE, Rafael JA, Skinner JA, Brown SC, Potter AC, Metzinger L, Watt DJ, Dickson JG, Tinsley JM, Davies KE. Utrophin-dystrophin-deficient mice as a model for Duchenne muscular dystrophy. Cell 1997; 90(4):717-27; http://dx.doi.org/10.1016/S0092-8674(00)80532-2
31. Grady RM, Teng H, Nichol MC, Cunningham JC, Wilkinson RS, Sanes JR. Skeletal and cardiac

myopathies in mice lacking utrophin and dystrophin: a model for Duchenne muscular dystrophy. Cell 1997; 90(4):729-38. PMID:9288752; http://dx.doi.org/10.1016/S0092-8674(00)80533-4

32. Deconinck N, Tinsley J, De Backer F, Fisher R, Kahn D, Phelps S, Davies K, Gillis JM. Expression of truncated utrophin leads to major functional improvements in dystrophin-deficient muscles of mice. Nat Med 1997; 3(11):1216-21. PMID:9359695; http://dx.doi.org/10.1038/nm1197-1216
33. Rafael JA, Tinsley JM, Potter AC, Deconinck AE, Davies KE. Skeletal muscle-specific expression of a utrophin transgene rescues utrophin-dystrophin deficient mice. Nat Genet 1998; 19(1):79-82. PMID:9590295; http://dx.doi.org/10.1038/ng0598-79
34. Squire S, Raymackers JM, Vandebrouck C, Potter A, Tinsley J, Fisher R, Gillis JM, Davies KE. Prevention of pathology in mdx mice by expression of utrophin: analysis using an inducible transgenic expression system. Hum Mol Genet 2002; 11(26):3333-44. PMID:12471059; http://dx.doi.org/10.1093/hmg/11.26.3333
35. Tan N, Lansman JB. Utrophin regulates modal gating of mechanosensitive ion channels in dystrophic skeletal muscle. J Physiol 2014; 592(Pt 15):3303-23; PMID:24879867; http://dx.doi.org/10.1113/jphysiol.2014.274332
36. Suchyna TM, Markin VS, Sachs F. Biophysics and structure of the patch and the gigaseal. Biophys J 2009; 97(3):738-47; PMID:19651032; http://dx.doi.org/10.1016/j.bpj.2009.05.018
37. Schmidt D, del Mármol J, MacKinnon R. Mechanistic basis for low threshold mechanosensitivity in voltage-dependent K+ channels. Proc Natl Acad Sci USA 2012; 109(26):10352-7; PMID:22675122; http://dx.doi.org/10.1073/pnas.1204700109
38. Ursell T, Agrawal A, Phillips R. Lipid bilayer mechanics in a pipette with glass-bilayer adhesion. Biophys J 2011; 101(8):1913-20; PMID:22004745; http://dx.doi.org/10.1016/j.bpj.2011.08.057
39. Huang H, Bae C, Sachs F, Suchyna TM. Caveolae regulation of mechanosensitive channel function in myotubes. PLoS One 2013; 8(8):e72894; PMID:24023653; http://dx.doi.org/10.1371/journal.pone.0072894
40. Schlörmann W, Steiniger F, Richter W, Kaufmann R, Hause G, Lemke C, Westermann M. The shape of caveolae is omega-like after glutaraldehyde fixation and cup-like after cryofixation. Histochem Cell Biol 2010; 133(2):223-8; PMID:19851779; http://dx.doi.org/10.1007/s00418-009-0651-8
41. Hamill OP, Marty A, Neher E, Sakmann B, Sigworth FJ. Improved patch-clamp techniques for high-resolution current recording from cells and cell-free membrane patches. Pflugers Arch 1981; 391(2):85-100. PMID:6270629; http://dx.doi.org/10.1007/BF00656997
42. Box B, Jenkins G. Time Series Analysis: Forecasting and Control. San Francisco, CA: Holden-Day; 1976.
43. Porta M, Diaz-Sylvester PL, Neumann JT, Escobar AL, Fleischer S, Copello JA. Coupled gating of skeletal muscle ryanodine receptors is modulated by Ca^{2+}, Mg^{2+}, and ATP. Am J Physiol Cell Physiol 2012; 303:C682-97; PMID:22785120; http://dx.doi.org/10.1152/ajpcell.00150.2012